Journal of Cultural Heritage 58 (2022) 156–166

Contents lists available at ScienceDirect

Journal of Cultural Heritage

journal homepage: www.elsevier.com/locate/culher

A smartphone-based innovative approach to discriminate red pigments in roman frescoes mock-ups

Roberto Sáez-Hernández[a], Kevin U. Antela[a], Gianni Gallello[b,*], M. Luisa Cervera[a,*], Adela R. Mauri-Aucejo[a]

[a] Universitat de València, Department of Analytical Chemistry. C/ Dr. Moliner, 50, Burjassot 46100, València, Spain
[b] Universitat de València, Department of Prehistory, Archaeology and Ancient History. Av. Blasco Ibañez, València 46010, Spain

ARTICLE INFO

Article history:
Received 5 May 2022
Accepted 3 October 2022
Available online 17 October 2022

Keywords:
Roman *fresco*
Smartphone
Spectroscopy
Mock-up
Pigment
Colorimetry

ABSTRACT

The characterization of red pigments in *frescoes* wall paintings has been of great interest for researchers to better understand raw material procurement dynamics, pigment receipts, stylistic evolution and to assess their conservation state. In this study a non-destructive colorimetric approach implementing a smartphone-based method was developed in order to be able to distinguish between three pigments made from minium, haematite and cinnabar minerals, and also mixed pigments, preparing *frescoes* mock-ups following the roman receipt described by Vitruvius. Portable FT-IR, Raman spectroscopy, portable XRF and visible reflectance spectra analyses were carried out as reference methods for smartphone colorimetry results validation. Employing a reference colour sheet to control changing lighting conditions, different chemometric approaches have been developed and tested, cross-referencing standard analytical results with the data obtained by smartphone. Overall, using only colour parameters from the smartphone, a Linear Discriminant Analysis and a Support Vector Classifier were tested to efficiently classify each sample based on the red pigment used, with low prediction errors. This work shows the potential of smartphones as cheap, fast and user-friendly analytical devices for the screening of frescoes, and as a prior selective step before carrying out further more expensive and specialized analyses.

Abbreviations

B.C.E.	Before common era
C.E.	Common era
Dim.	Dimension
FT-IR	Fourier-transform infrared
kNN	k-Nearest neighbours
LDA	Linear Discriminant Analysis
LOD	Limit of detection
LOOCV	Leave one out cross validation
PCA	Principal Component Analysis
p-XRF	Portable X-ray Fluorescence
ROI	Region Of Interest
SNV	Standard Normal Variate
SVC	Support Vector Classifier

Introduction

Roman wall paintings and frescoes studies have been carried out to deal with raw material characterization, pigment receipts, stylistic evolution and conservation issues. Therefore, stylistic and macroscopic studies together with non-destructive or minimally intrusive analytical techniques have been developed to preserve these unique remains [1].

From the analytical point of view, portable X-ray fluorescence (p-XRF) and Raman spectroscopy have been the most used techniques to identify pigments' composition in roman frescoes. Some works, like those of Tuñón et al. [2] and Boschetti et al. [3], investigated Roman Republic painted mosaics using the aforementioned devices, and were able to identify different inorganic pigments used to obtain pink, blue, and different yellow hues. Romani and collaborators [4] were studying S. Nicola in Carcere (Italy) wall painting, combining XRF, Raman and UV–Vis-SWIR (Ultraviolet-Visible-Short Wave Infrared) to identify the colour palette used. Finally, Roman pigments in the Vesuvian area were analysed using

* Corresponding authors.
E-mail addresses: roberto.saez@uv.es (R. Sáez-Hernández), kevin.urbano@uv.es (K.U. Antela), gianni.gallello@uv.es (G. Gallello), m.luisa.cervera@uv.es (M.L. Cervera), adela.mauri@uv.es (A.R. Mauri-Aucejo).

https://doi.org/10.1016/j.culher.2022.10.003

Raman spectroscopy and XRF to describe and identify the origin of inorganic pigments preserved in the Archaeological Park of Pompeii [5].

Fourier-transform infrared (FT-IR) spectroscopy is also used to assess the presence of organic compounds, such as those present in varnishes and binders. Prieto-Taboada et al. [6] analysed the blue pigments found in the Pompeian walls of Ariadne's house, identifying the raw material used and the environmental degradation compounds by combining FT-IR, Raman and XRF analyses.

Finally, the interest in running colorimetric analyses of pigments is due from the information provided by the reflected light on the painted surface, which mainly depends on the chemical specie absorbing the light, expressed either as a reflectance/absorption spectrum or as colour parameters. The three coordinates representing the colour observed in given lighting conditions constitute a colour space, being CIE L*a*b* and CIE L*h*C* widely known. Both of them share the lighting coordinate (L*), which represents lightness in a gradient ranging from 0 (darkest) to 100 (lightest), and two colour coordinates representing the chromatic characteristics of the colour. For CIE L*a*b* colour space, a* represents the change from green to red, and b* the change from blue to yellow (both ranging from −120 to +120) [7]. The colour coordinates of CIE L*h*C* represent colour in polar coordinates: h* (hue) represents the angle, and C* (chromaticity) represents the dimension of the vector [8].

Pigments' colorimetric analyses have already been employed to identify different chemical species [9]. For example, Egyptian green and blue pigments [10], 16th century pigments [11], yellow [12], and Persian red pigments [13] were analysed by colorimetric methods, providing useful information for their characterization.

During the last decades, the development of colorimetric methods based in smartphone technology has become more and more common [14,15]. Thus, applications in environmental studies [16–18] and food analysis are widely used [19–21]. However, in the field of Cultural Heritage, just a few works have been published proposing a methodological approach based on smartphone devices [22]. The main advantages of using smartphones as analytical devices are their wide availability, their low cost and the user-friendly interfaces. These characteristics end up being very useful for a first screening [22] of the sample, to select subsamples or areas of *frescoes* worth to be studied before using more costly, time consuming and sophisticate analytical tools. Nonetheless, since they are not originally designed for analytical purposes, specific methodological approaches need to be developed to control light influence and environmental conditions.

Due to the high interest in roman frescoes for the specialists in the field, and the difficulty in running analytical tests in original artworks, experimental approaches in the literature employing mock-up samples are found. Piovesan et al. developed a microstratigraphic analytical approach to distinguish between the fresco and lime-painting techniques using microscopy and spectroscopy analytical methods [23]. Similarly, the alteration of mercury-based red pigment cinnabar (HgS) was assessed in an experimental approach by Neiman and colleagues [24]. To do it, different salt concentrations and light exposure conditions were applied to a wall replica and different analyses including colorimetric ones were carried out. Also, Regazzoni et al. [25] developed microscopy methods for Romanesque style wall paint replicas using microstratigraphic studies.

In this work, experimental *frescoes* were characterised with non-destructive analytical techniques such as p-XRF, FTIR and Raman, together with a spectrocolorimeter employed as reference methods for setting up the smartphone application. Finally, the obtained data were statistically processed and the chemical information cross-referenced with smartphone images to identify and classify the studied pigment replicas.

Research aim

This study aims to develop an analytical strategy to determine red colours made of different compounds in roman frescoes based on smartphone image analysis and chemometrics. To it, frescoes replicas were built following the original recipes and painted with three different red pigments (haematite, minium and cinnabar). A full palette of red hues with pure pigments and mixtures was obtained and analysed by standard non-destructive spectroscopic techniques such as portable X-ray fluorescence, Fourier Transform Infrared spectroscopy, Raman spectroscopy and visible reflectance spectroscopy. These results were cross-referenced with the image parameters obtained by smartphone to evaluate its capability in discriminating between pigments, and to observe the reliability of the results obtained compared with more standardized analytical approaches. Furthermore, different statistical classification strategies were proposed based on image parameters, Linear Discriminant Analysis (LDA), Support Vector Classifier (SVC) and k-Nearest Neighbours (kNN). These are well-established statistical methods [26] extensively used in the field of chemical analysis [27–29] especially due to the their applicability in many different field of studies. Here, the data were processed employing different data processing approaches to evaluate which one is the most suitable in this study and which one better enhances the quality of the obtained data.

Overall, this paper develops a completely new strategy to analyse and characterize frescoes red pigments based on smartphone colorimetry validated with reference methods. With it, a fast and easy method is proposed to obtain valuable chemical information which can be used as a first insight for cultural heritage research, conservation and restoration efforts, posing the base to the development of a mobile application for red pigments characterization.

Material and methods

Frescoes replicas preparation

During the roman times, structures and edifications were usually made out of bricks, pebble, or sun-dried mud covered with mortar (a mixture of sand and lime in different proportions). Usually, a layer of lime was applied in the wall surface and its width depended on the period, area, or economic capabilities, and it was often mechanically polished to obtain a smooth surface, which could also be used as a base for the painting [30].

Wall paintings have been recorded since the palaeolithic, but Egyptians first developed a technique to apply a preparatory layer before the application of the pigments [31]. However, It was during the roman period (II B.C.E. - III C.E. centuries) that a major technical apogee took place [31]. Despite the fact that mortar manufacturing processes depend on the time span and location, some characteristics are common to all the studied materials.

A detailed description of the procedures, materials and pigments commonly employed amongst builders and artists can be found in the *De Architectura Libri X*, written by Vitruvius (20 BC.E). The writer indicates that mortar was made with 2 parts of river sand, and one part of dead lime, stating that 6 different layers should be applied: starting from an initial coarse plaster, up until a fine lime layer. For this last layer, the author recommended to include 4 layers of sequentially finer and finer marble and mortar to stabilize the surface [31].

However, in most of the cases, only two or three layers were reported by several studies. The first one was a mixture of sand and lime in a 2:1 or 3:1 proportion, and 3 and 5 cm width, while

the second one was an outer layer of pure lime with 1–10 mm width [30–32].

Regarding the pigment, it was usually applied using different methods, giving place to a range of techniques such as *fresco, secco and mezzo fresco*. The main difference amongst those was the state of the pigment and the degree of humidity of the wall. If the water-suspended pigment was applied in a partially dried wall, the technique would be *fresco*; if suspended in a lime-water solution, and applied to a dried wall, the technique would be called *secco*. For these techniques, the binder (substance which allowed the pigment to stick to the wall) was the $CaCO_3$ formed from reaction of lime (CaO) with atmospheric CO_2. Nonetheless, some organic binders like bee wax, wheat paste and egg were also used [33].

Amongst a wide variety of roman *frescoes* characteristic colours, red was one of the most used ones. As described in the literature haematite, a common iron oxide compound (Fe_2O_3), minium (also known as red lead, Pb_3O_4) and cinnabar (the common source for elemental mercury) were the most important minerals employed by the romans.

Haematite has been identified by several studies [6,9,31,34], including as a solid pigments ready to be used in the Vesuvian area before the eruption [5]. This compound was one of the mentioned red species in the VII chapter of Vitruvius work [35]. Minium was less frequently employed than haematite, but it can be also found in red parts of roman *frescoes* [9,31]. Finally, the use of cinnabar in roman painting was identified just in some specific cases [5,24,36,37], probably due to its higher cost.

These pigments were used either as a pure compound, or applied as a mixture with other red species to obtain different colour nuances. For instance, a combination of iron red (haematite) and lead red (minium) was identified in Grau Vell site, the ancient roman harbour of Sagunto, Spain [32].

In this work, *frescoes* mock-ups were prepared based on the recipe described by Vitruvius and Piovesan et al. [23].

First, sand (35.3 ± 0.7% SiO2) and lime (CaO + MgO > 95%; MgO < 2.5%, CO2 < 3%) were acquired in a specialized retailer, and the sand was sieved (<1 mm) in order to separate coarse from fine sand. Haematite (Ref.: #48,651), minium (Ref.: #42,500) and cinnabar (Ref.: #10,620) pigments were acquired at Kremer pigment *via* Agaragar (https://agaragar.net/).

A ceramic tile was employed as a support (20 × 30 × 0.5 cm, containing Al, Si and Ca as major elements), being humidified in advance using a wet brush to ease the adhesion of the mortar layers. Successively, a first layer was added, consisting of coarse sand and lime in a 3:1 proportion. Water to reach a correct consistency was added to the mixture and then it was mechanically flattened. This first layer was left to dry. Later, a second layer of mortar consisting in a mixture of fine sand and lime in a 3:1 proportion was added and left to dry again until enough $CaCO_3$ had formed. Lastly, a final layer of pure lime suspended in water was applied to the surface and left to dry, after which, the pigments suspended in water were applied.

Two different types of samples consisting in pure pigments (either haematite, cinnabar or minium) and mixed pigments (different combination and proportions of haematite, cinnabar or minium) were prepared. When working with pure pigments, an amount ranging from 0.2 to 0.8 g of each pigment was suspended in 1 mL of water, to obtain different graduation of colours. For mixtures, six different pigment combinations were prepared in a total of 1 mL of water. Table 1 summarizes the different types of samples and a detailed identification of the colours gradient can be seen in **Supplementary Table 2.**

The prepared pigments were applied on the support in different proportions and brush strokes intensities to obtain diverse colour hues (**Supplementary Figure 1**). Regarding the mixtures, five different colour spots were painted. Once applied in the surface, the pigments were left to dry for 4–5 days and then, finally measured by the different analytical techniques.

Table 1
Composition of the samples under study.

Type	Sample	Composition
Pure	*Haematite*	*Pure haematite in different amounts*
Pure	*Minium*	*Pure minium in different amounts*
Pure	*Cinnabar*	*Pure cinnabar in different amounts*
Mixture	*0.2Fe_0.6Hg*	*0.2 g haematite + 0.6 g cinnabar*
Mixture	*0.6Fe_0.2Hg*	*0.6 g haematite + 0.2 g cinnabar*
Mixture	*0.2Fe_0.6Pb*	*0.2 g haematite + 0.6 g minium*
Mixture	*0.6Fe_0.2Pb*	*0.6 g haematite + 0.2 g minium*
Mixture	*0.2Hg_0.6Pb*	*0.2 g cinnabar + 0.6 g minium*
Mixture	*0.6Hg_0.2Pb*	*0.6 g cinnabar + 0.2 g minium*

Raman analysis

A portable Raman spectrometer (i-Raman® Plus spectrometer (model: BWS465–785S) by B&W Tek) was employed to directly measure the samples using a fibre probe. The laser wavelength was 785 nm, with a total laser power of 340 mW (used at 15%), integration time 1000 ms and 20 scans per measurement. The obtained spectra were corrected for baseline effects in the software (BWSpec®) with the baseline removal, setting the correction parameter (λ) at 36.

FT-IR analysis

Infrared spectra were obtained employing a 4300 Handheld FTIR from Agilent, with diffuse reflectance accessory in the range of 650–4000 cm^{-1}, using a spectral resolution of 4 cm^{-1}. Each sample was acquired with 50 scans, and a blank measurement between each analysis was made using the coarse gold reference cap.

p-XRF analysis

X-Ray fluorescence analysis was carried out using a S1 Titan analyser from Bruker 500S. Elements above the limit of detection (LOD) of the instrument were taken into consideration, and quantified as mass percentage using the GeoChem Trace internal calibration, in the form of: MgO, Al_2O_3, SiO_2, P_2O_5, S, Cl, K_2O, CaO, Fe, Ni, Cu, Zn, As, Rb, Sr, Zr, Hg, Tl, and Pb.

Colorimetric characterization of the replicas

Colour was captured using a spectrocolorimeter from Konica Minolta CM-26d, in the region of 400 −740 nm with a resolution of 10 nm. The illuminant was D65, the light source was a pulsed xenon lamp, and data from CIE L*a*b* and CIE L*h*C* were extracted. Prior to the measurements, the device was calibrated using the references white and black provided by the manufacturer. To further ensure that the device was correctly calibrated, the white reference was measured to check that a (L*, a*, b*) ≈ (100, 0, 0) was obtained. Three different measurements of the colour of each painted spot were captured and averaged.

Regarding the colorimetric smartphone analysis, a Samsung Galaxy Edge S7 model SM-G93F, with a 12.2 MP camera sensor was used. Photos were taken in the native camera app in automatic mode, with a distance of 21 cm to the samples, and completely parallel to them. Focus was made on one of the parts of the reference colour sheet (ColorChecker Classic Mini, from X-Rite Pantone, 24 colours, 57 × 86 mm, containing both greyscale and chromatic colours). The images files in .jpg format were transferred to Matlab to carry out the image treatment.

Colour parameters were obtained using both devices as capturing devices. While the spectrocolorimeter provided both reflectance spectra and colour parameters in the CIE L*a*b* colour space, the smartphone only provided RGB colour parameters. The signal obtained with the smartphone was corrected as described in the *Image treatment process* section.

Image treatment process

Using Colorlab tool [38], 3 different regions of interest (ROI) were selected from each sample, and the average value was considered as representative. RGB (as the smartphone saves information in this colour space) values were converted to CIE L*a*b* and CIE L*h*C* using the white reference from the colour sheet with the built-in functions of the Matlab tool.

To compensate the lighting conditions effect, the colour sheet was previously measured using the spectrocolorimeter, and a calibration was obtained to convert and correct CIE L*a*b* smartphone data. This conversion was based in a linear regression model, which was applied to the L*a*b* values obtained by the smartphone. A detailed description of the data treatment procedure was reported in **Supplementary Figure 2**). For a detailed description of how to implement this procedure, please check the Supplementary materials' section "Implementation detailed description".

Statistical analysis

Statistical analysis was carried out by R sofware [39] using *factoextra* [40], *MASS* [41], *e1071* [42], *class* [41] and *FactoMineR* [43] packages for multivariate analysis. Visual representation of the data was made using *ggplot2* [44] while the package *signal* [45] was used in the spectral treatment step.

Principal Component Analysis (PCA) was employed to study pXRF and Colorimetric data including all the measured points. By this statistical method, a reduction in the number of variables is obtained while retaining most part of the variability of the original dataset [46]. By this methodology, new variables/dimensions (called Principal Components) are generated on the basis of the linear combinations of original variables. In this work, each one of these new dimensions have been called "*Dim.*" and only the first few dimensions are used, since they contain most of the valuable information from the dataset.

Spectral treatment of the reflectance spectra in the visible range to carry out Principal Component Analysis was done using centred spectral data (not scaling variance, to avoid giving more importance to background noise) in the range from 530 nm to 740 nm. Regarding the pXRF data, the elemental composition obtained was used as an input for the PCA model.

In order to apply and optimize a proper statistical approach to distinguish between different pigments, three different classification methodologies have been applied and compared: k-Nearest Neighbour (kNN), Linear Discriminant Analysis (LDA) and Support Vector Classifier (SVC) and the results have been validated using cross validation.

These classificatory methods are based on different statistical principles: LDA works by studying the distribution of each one of the categories and creating new linear discriminant functions separating them [47]; kNN classifies new samples on the basis of the class to which its neighbours belong [27]; and last, SVC creates borders, both linear and non-linear (margins), between groups trying to minimize the error committed [29]. Since these methods work in different ways, they have been compared in order to assess their performances in this case study. In all cases, the dataset was randomly split into calibration and test sets to assess the validity of each methodology.

Results and discussion

Spectroscopic characterization

Characteristic Raman spectra were obtained for haematite at 288 and 405 cm^{-1}, minium at 392, 549 and 1085 cm^{-1} and cinnabar at 251 and 344 cm^{-1}. These peaks were also identified in the mixed samples present in the mock-ups (**Supplementary figure 3**).

Supplementary figure 4 shows the FT-IR reflectance spectra for each one of the pigments and the mortars' surface. Standard Normal Variate (SNV) was applied in order to make up for the scattering effect between different measurements as recommended in the literature [48], and a Savitzky-Golay (SG) smoothing filter (order 1, window 15) was used to correct the noise. The results indicate that a *reststrahlen* band is observed at 1400 cm^{-1}, corresponding to the intense absorption band of the CO_3^{2-} at that same wavenumber [49]. Additionally, two intense bands at 1750 and 2500 cm^{-1} are observed, which might correspond to amplified overtones and combination bands of $CaCO_3$ [50,51]. More specifically, the band around 1750 cm^{-1} is due to the overtone of the out-of-plane bending of CO_3^{2-} group [52], while the band around 2500 cm^{-1} is generated as a combination of two bands (the one around 698–745 cm^{-1} plus the main one around 1450 cm^{-1}) [53]. These appear as very subtle signals in transmittance mode [49], and get amplified as a consequence of the utilization of reflectance mode [54]. These spectra corresponded to the presence of $CaCO_3$ and no signal attributed to the pigments was found. As can be observed in the **Supplementary figure 5,** FT-IR results were not able to show differences between the studied pigments, and the presence of $CaCO_3$ in all the measured samples is due to the carbonation process taking place during the manufacturing of the support.

p-XRF analysis

Supplementary figure 6 shows the pXRF obtained results of CaO, Fe, Pb and Hg for all the different painted spots (the minor elements are summarized in **Supplementary Table 1**). Fe content is between 0 and 25% (w/w) in haematite, Pb reached up to a 50% in minium, while Hg 60% in one sample. The content of CaO is higher or lower depending on the pigment concentration. An exploratory analysis of the samples using principal components analysis (shown in Fig. 1) shows three main clusters based on the elemental composition: most of the minium samples are located on the positive direction of *Dim.*1 and *Dim.*2; haematite samples are in the negative direction of *Dim.*2 and cinnabar ones are found on the positive *Dim.*1 direction, corresponding to the right bottom part of the plot. PCA loadings show that Fe is correlated to Al, Si, and Cu, and Pb is correlated to Ni, Zr, As and Cl, while Hg is tightly correlated to Sr, Tl, Zn, P and Rb. Regarding S, it is expected to appear in the cinnabar samples (HgS). However, it is also present in the samples painted with minium probably due to the presence of PbS, in this last pigment. Looking at the different mixtures samples (Fig. 1**b**), the results are similar to the previous case being the main elements of the most abundant pigment driving the samples location in the plot.

Colorimetric characterization

Pigments were characterized using the reflectance spectra in the visible range and **Supplementary figure 7** shows the obtained spectra for both the pure pigments and the mixtures, as well as their first derivatives. It can be observed that minium is reflecting light at a lower wavelength, which implies that it will have more yellow component when compared to the other three pigments. Interestingly, as seen in the two peaks obtained in the derivatives,

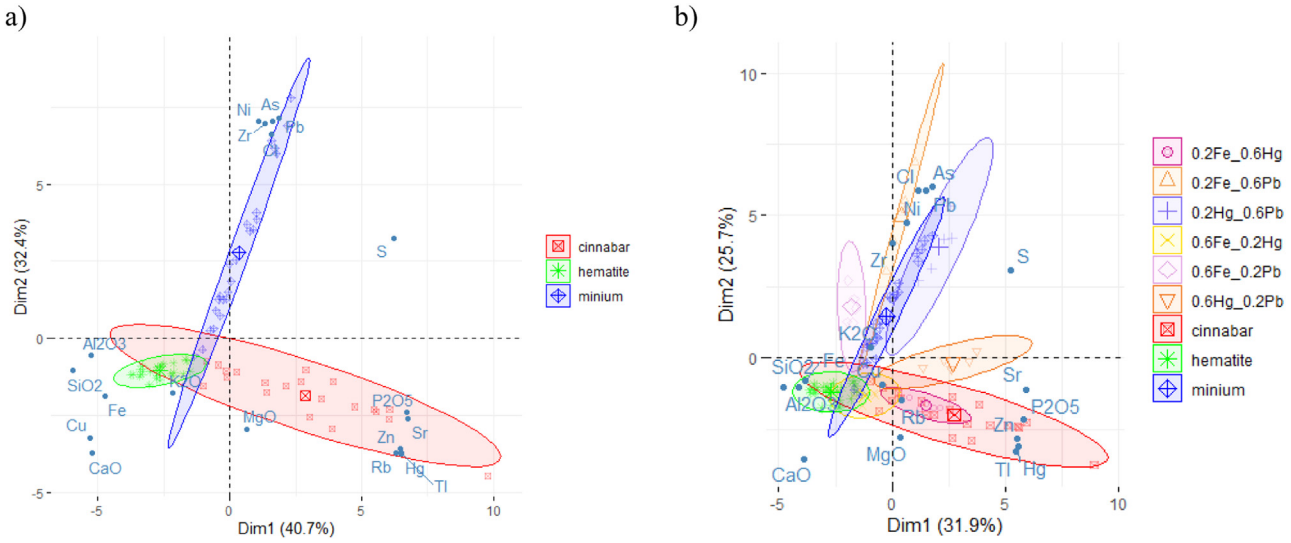

Fig. 1. PCA biplot exploratory analysis for the elemental composition of (a) pure pigments. (b) pure and mixtures spots, based on p-XRF.

haematite showed two inflection points, a differential property from the other pigments. Assessing the studied mixtures, it can be seen that the resulting spectra is most similar to the one obtained for the pure pigment which represents the major part of such mixture. For those cases in which haematite is present, its influence seems more important, as can be seen in the cases of 0.2Fe_0.6 Pb and 0.2Fe_0.6Hg: even though haematite is in a smaller concentration in these samples, the resulting spectra is more similar to pure haematite rather than to pure minium or cinnabar, respectively. This fact can be seen in the PCA scores plot (Fig. 2**)**.

It can be observed that all the samples containing Fe (either as a major or as minor constituent) fall closer to the pure haematite cluster. On the other hand, Pb and Hg mixtures present more spectral differences. Additionally, it can be observed that minium is differentiated from the other two pigments based on spectral differences around 550–570 nm. This is in good accordance with the visual analysis of the reflectance spectra. Some samples are dispersed and away from the centre of their corresponding clusters. That is the case for samples labelled as "*PP10*", "*PR11*", "*PR21*", "*PR25*" and "*PC18*". As can be seen in **Supplementary table 2**, these samples present a very low pigmentation, thus reflecting much of the light due to the major white component of the colour.

Regarding the colorimetric analysis of the samples using smartphone, the obtained colour parameters in both CIE L*a*b* and CIE L*h*C* are shown in Fig. 3**.**

The lightness parameter, L*, shows that haematite is generally less lightful than the other two pigments, while minium is the one with the most lightness and less dispersion of data. Minium and cinnabar share an important range of L* values. Regarding the a* parameter (which represents how red the sample is), cinnabar is the reddest from all three, while haematite is the least red. However, all three pigments fall in similar areas comprising similar a* values. Mixtures of Hg and Pb were exacerbating the red aspect of the spot, while samples with 0.6 g of Fe were the least red mixtures.

For the b* parameter, it was minium which had a higher b* value (which represents the change from blue to yellow), due to the presence of more yellow component. This is a distinguishing characteristic, causing that a sample with minium increases its b* component in comparison to the pure pigment. This result is also in good accordance with the spectral properties described in **Supplementary figure 7.**

Regarding C* and h* parameters, it can be seen that C* behaves very similarly to b*, being minium the most colourful pigment of all three. Hue, h* -which represents the angle from pure red to pure yellow-, proved that minium was the pigment which had the highest component of yellow, followed by haematite.

Overall, the colorimetric analysis proves that minium is the most different pigment, and haematite and cinnabar are similar to one another, although they can be discriminated based on the L* component.

Cross-referencing the data from the p-XRF with CIE L*a*b* colorimetric parameters from the smartphone through a PCA, colorimetric information and elemental information were correlated (**Supplementary figure 8**). Dimensions 2 and 3 were selected because *Dim.*1 was highly influenced by non-discriminating parameters S and CaO (around 20% of the explained variance of this component was attributed to them). Firstly, it proves that samples with higher concentrations of lead in them had higher values of b*. Additionally, the concentration of CaO was opposite to increased value of a* and correlated to increased L*, proving that as more pigment is visible, less lime surface is left.

Identification of the pigment based on chemometrics and image analysis

As can be deduced from the previous results description, these three red pigments have some differential colorimetric characteristics that might allow to discriminate them on the basis of the colour parameters obtained with the smartphone. To it, three different classification methodologies have been used: k-nearest neighbours (kNN), a Linear Discriminant Analysis (LDA) model, and a Support Vector Classifier (SVC). All three techniques have been compared in terms of simplicity and prediction error.

k-Nearest neighbours (kNN)

Using colorimetric CIE L*a*b* data obtained with the smartphone, after calibrating it as stated in *Image Treatment Process* section, a kNN classification procedure was carried out. kNN classification is a supervised classification method which assigns a specific sample to a certain group, based on its distance to the *k*-nearest calibration point(s) which have been previously used to build the model. After optimization (**Supplementary figure 9**), the dataset

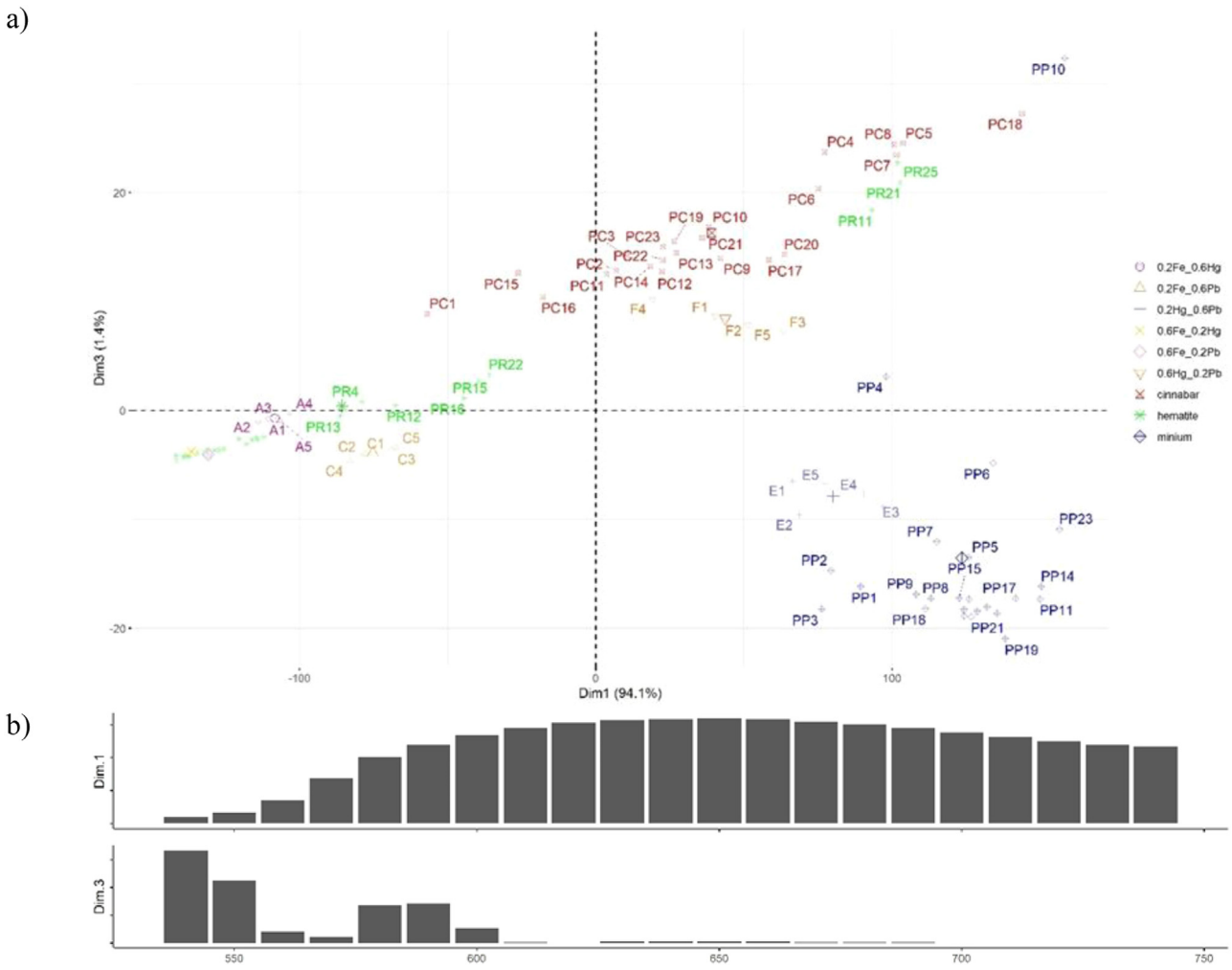

Fig. 2. (a) Scores plot for the PCA of the spectral data (centred) from 530 to 740 nm obtained with the spectrocolorimeter (Dim. 1 and Dim. 3). (b) contribution of each variable (wavelength) to the different dimensions.

was divided into a 80:20 ratio (calibration:test) to assess the degree of applicability of the chemometric technique.

Regarding the analysis of only pure samples, a calibration set of 58 samples (80% of the total dataset) was randomly chosen for 100 times to build 100 different kNN classification models. Each one of them was applied to classify the test set built with the 15 samples which were not included in the calibration step. A prediction error (estimated as the number of times for which the predicted assignment was different from the real one) was computed each time, and an average value of the 100 runs was computed using $k = 3$ (as can be seen in **Supplementary figure 9 (c.1)**). The average error of prediction was 14 ± 9%. Hence, ten different models were carried out as stated above to visualize the mistakes, and the results are plotted in **Supplementary Table 3**. In this example, 13 times minium and haematite were wrongly predicted; 9 times cinnabar and haematite, and only once minium was confused by cinnabar.

When it comes to the mixtures of different red pigments, the model was built in the same way (splitting the dataset into 80:20 proportions) and repeating it for 100 times to obtain an averaged error value. In this case, since the total dataset contained 103 samples, the calibration set consisted of a random selection of 82 samples, and the test set had 21. As is deduced from **Supplementary figure 9 (c.2)**, a $k = 1$ was chosen. The error of prediction found was 12 ± 8%, very similar to the result obtained in the case when only pure samples were considered. Once again, 10 different models were created and evaluated, showing the results in **Supplementary Table 4**. The results here indicate that the inclusion of mixtures in the dataset does not significantly affect the classification, obtaining a similar error of prediction for the 100 tries. Additionally, mixture samples were correctly identified with the proposed classifier.

Linear discriminant analysis (LDA)

LDA is another classifying chemometric technique which looks for discriminant functions or vectors, that is, linear combinations of the variables which maximize the variance inter-categories at the time that it minimizes the variance intra-categories [55].

Firstly, the whole dataset was separated into calibration (consisting in the pure pigments), and test (mixtures).With this, the degree of similarity of each mixture to the pure pigments is assessed. The calibration set consists of a (73 × 4) matrix (73 different pure pigment samples as rows; label, L*, a* and b* as columns). Since only three response categories (levels) are added in the calibration step as labels, the response of the model will be to classify the different mixtures either as haematite, minium or cinnabar. Table 2 shows the confusion matrix obtained for this test:

The results indicate that *0.2Fe_0.*6 Hg is partially classified as haematite and cinnabar. Interestingly, its counterpart (*0.6Fe_0.*2 Hg) is only classified as haematite. This is indicating, as was already seen in the previous plots, that haematite is having a major influence on the final aspect, and hence the mixture

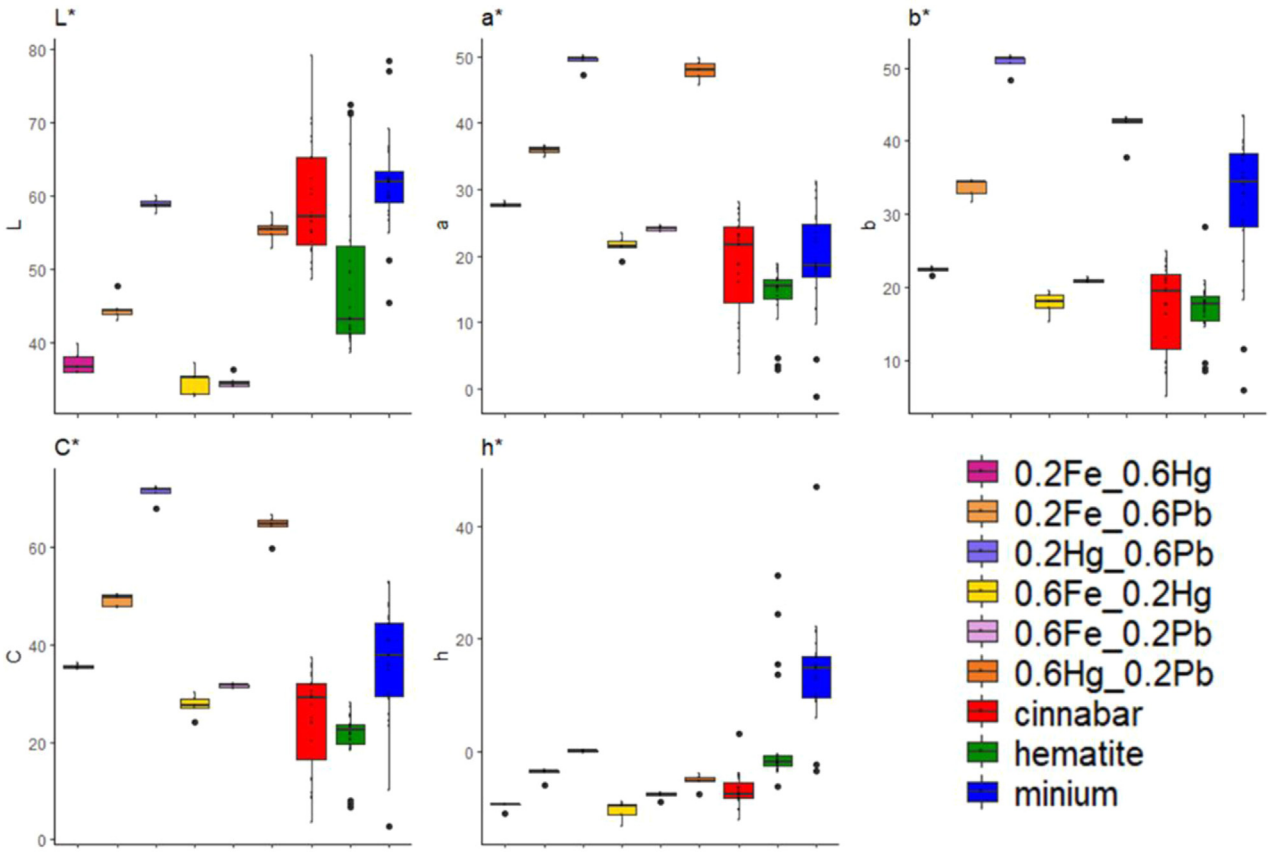

Fig. 3. Boxplot showing the colour parameters obtained with the smartphone. Each box comprises the data from the 1st to the 3rd quartile. The median of each data subset is represented by a flat line. Samples are represented, from left to right, in the order specified in the legend.

Table 2
Confusion matrix for the LDA model created with pure pigments as calibration and mixtures as test samples. Smartphone colorimetric data of CIE L*a*b* colour space.

Real	Classified as Cinnabar	Haematite	Minium
0.2Fe_0.6Hg	3	2	0
0.2Fe_0.6Pb	5	0	0
0.2Hg_0.6Pb	5	0	0
0.6Fe_0.2Hg	0	5	0
0.6Fe_0.2Pb	0	5	0
0.6Hg_0.2Pb	5	0	0

0.2Fe_0.6 Hg is partially read as haematite. Regarding the Fe and Pb mixtures, it is interesting that *0.2Fe_0.6* Pb is classified as cinnabar, despite not containing cinnabar in it. A PCA (*Dim.2* and *Dim.3*) of the CIE L*a*b* colorimetric data, shown in Fig. 4, proves that these mixtures are half way through the cinnabar and haematite clusters, causing the confusion: even though these samples contain a higher amount of minium (which should increase the b* value, and thus take them down in the negative *Dim.3* direction, mainly driven by b*), the resulting colour is not that yellowish. On the other hand, *0.6Fe_0.2* Pb is classified as pure haematite. Last, cinnabar and minium mixtures are classified as pure cinnabar in both cases, mainly driven by the darker and redder feature of the resulting sample (on *Dim.3* and *Dim.2* positive directions).

Next, the LDA model was carried out with all possible samples, and then the assigned class was computed. The model was built following a Leave One Out Cross Validation (LOOCV). To it, the model was built without a test sample each time, and the predicted category contrasted with the real one. Results are shown as a confusion matrix in Table 3. The model had an error of prediction of 7.77%. As can be seen, all mixtures were correctly classified in all cases, except for the *0.6Fe_0.2* Hg, which was confused once.

Regarding the pure samples, cinnabar is correctly classified in all cases, and some confusions arise when classifying haematite and minium: haematite is classified as cinnabar and as minium twice for each category. For the case of haematite, samples "*PR13*" and "*PR14*" are classified as minium samples due to a high b* component in these samples, while "*PR4*" and "*PR9*" are classified as cinnabar, since they present a higher a* value, a characteristic of cinnabar samples. Regarding the misclassified minium samples, "*PP6*" is set as cinnabar (as can be seen in **Supplementary Table 2**, it is a slightly coloured spot, and thus it has a low b* value), while "*PP4*", "*PP5*" and "*PP7*" are assigned as haematite.

Support vector classifier (SVC)

A support vector classifier is a chemometric tool which aims to classify different test samples into a given number of categories, depending on the side in which each observation will fall with respect to a separation plane, called the *soft margin*. To it, a calibration set is fed to build a model, allowing a certain degree of misses (the reason why the separation is based on a *soft* margin). This tolerance is often referred to as *cost*, and it is expressed as *C*. After, the test samples are classified as different categories depending on the area in which they fall [56]. In this case, since 3 categories are studied, a *one-vs-one* extension was used. In it, 3 different SVC are built, considering 2 classes in each case. Overall, each test sample is classified as the category to which it has been classified most frequently. Regarding the evaluation of the method, a k-fold cross validation was carried out. This method consists in splitting the

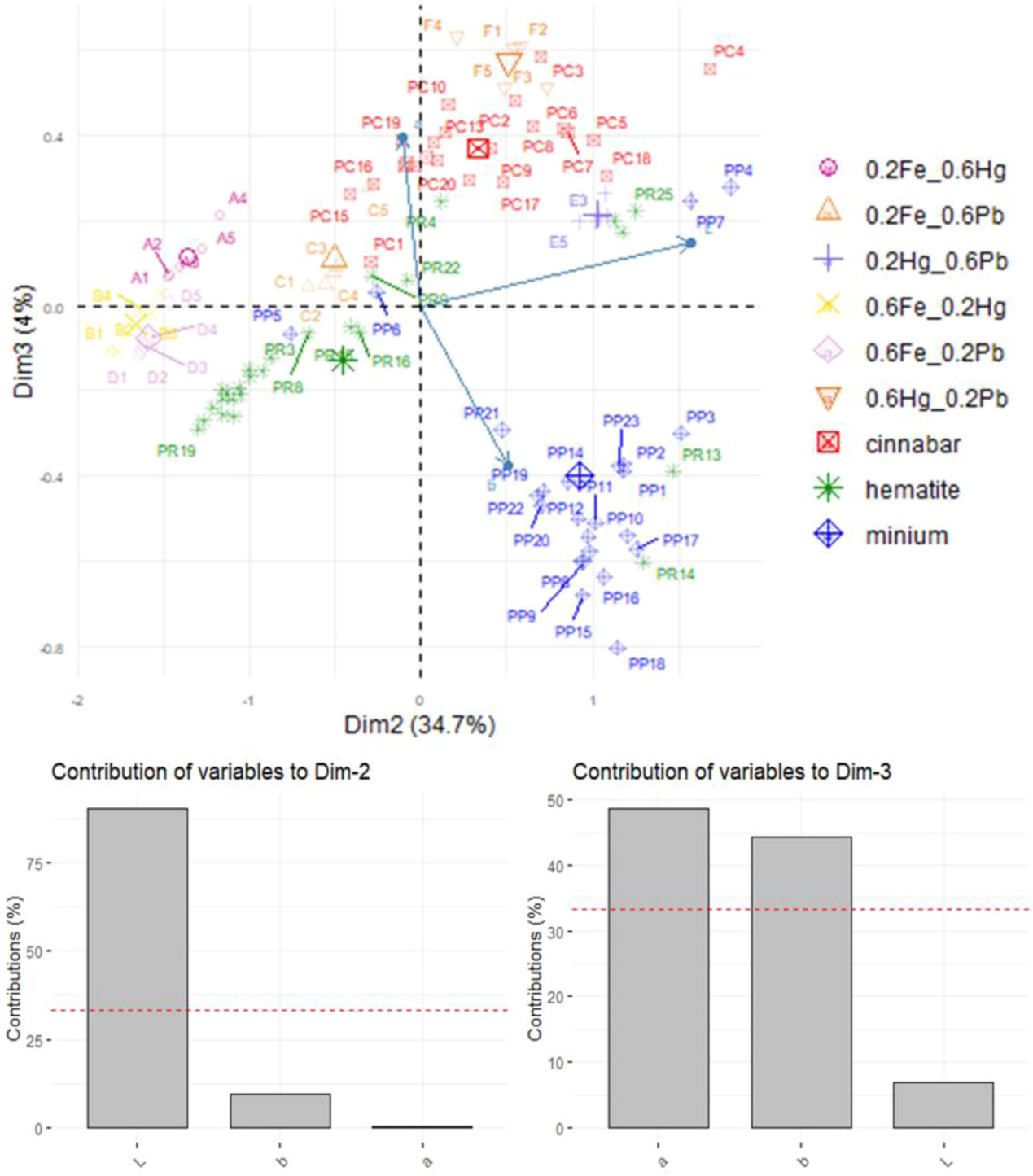

Fig. 4. PCA biplot (Dimensions 2 and 3) for the CIE L*a*b* smartphone data. The contributions of the variables to the principal components is shown.

dataset into *k* different groups with a similar number of observations, and using one of the groups as a test set.

As in the LDA model, two different models were built: first, pure samples were used to calibrate, and mixtures were predicted; and second, the whole dataset was used both to calibrate and predict.

Regarding the first model, $k = 10$ and $C = 1$ were used. Results are shown in Table 4. In this case, the 0.2Fe_0.6 Hg samples are fully classified as haematite. Unlike the case for LDA, the SVC does assign the sample 0.2Hg_0.6 Pb to minium, while the LDA classified it as cinnabar.

Evaluating the second model ($k = 1$, $C = 15$), in which the whole dataset was used, Table 5 summarizes the results. This time, only 7 out of the 103 samples are wrongly classified (6.80% error). Very similar results, in terms of misclassifications, are obtained when compared with LDA.

Spectrocolorimeter and smartphone classification performance

A comparison between the signals obtained with both devices can be seen in **Supplementary Figure 10**. A linear trend can be

Table 3
Confusion matrix for the LDA model created with pure pigments as calibration and mixtures as test samples. Colorimetric data of CIE L*a*b*.

Real	Predicted 0.2Fe_0.6Hg	0.2Fe_0.6Pb	0.2Hg_0.6Pb	0.6Fe_0.2Hg	0.6Fe_0.2Pb	0.6Hg_0.2Pb	cinnabar	haematite	minium
0.2Fe_0.6Hg	5	0	0	0	0	0	0	0	0
0.2Fe_0.6Pb	0	5	0	0	0	0	0	0	0
0.2Hg_0.6Pb	0	0	5	0	0	0	0	0	0
0.6Fe_0.2Hg	0	0	0	4	1	0	0	0	0
0.6Fe_0.2Pb	0	0	0	0	5	0	0	0	0
0.6Hg_0.2Pb	0	0	0	0	0	5	0	0	0
cinnabar	0	0	0	0	0	0	23	0	0
haematite	0	0	0	0	0	0	2	22	2
minium	0	0	0	0	0	0	1	3	20

Table 4
Confusion matrix for the SVC ($k = 10$, $C = 1$) model created with pure pigments as calibration and mixtures as test samples. Colorimetric data of CIE L*a*b*.

Real	Classified Cinnabar	Haematite	Minium
0.2Fe_0.6Hg	0	5	0
0.2Fe_0.6Pb	5	0	0
0.2Hg_0.6Pb	0	0	5
0.6Fe_0.2Hg	0	5	0
0.6Fe_0.2Pb	0	5	0
0.6Hg_0.2Pb	5	0	0

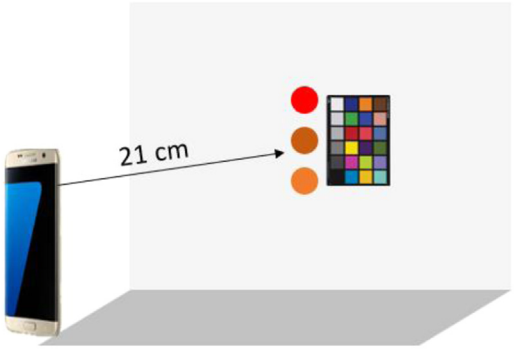

Fig. 5. Schematic representation of the proposed setup for the colorimetric identification of roman pigments in wall paintings.

observed, proving that the smartphone was registering colour proportionally with respect to the reference device.

LDA and SVC models built employing the smartphone data were compared with those of the portable spectrocolorimeter. Thus, the LDA model was created similarly with the CIE L*a*b* data obtained with the spectrocolorimeter, yielding 18.4% error of prediction. Regarding the SVC (in this case, the optimal model was obtained for a linear kernel with a C = 25), the algorithm provided 10.7% error of prediction. These results indicate that the error of prediction obtained with the smartphone was lower than the one obtained by using the spectrocolorimeter.

Although for both smartphone and spectrocolorimeter the data were obtained by extracting the colour of 3 different regions of interest of each coloured spot, the sampling process employing the spectrocolorimeter can be harder than the smartphone for samples which might be a little bit coarse. Since the spectrocolorimeter requires direct contact with the sample surface, any hollow between them can interfere with the final result.

Additionally, the contact between the spectrocolorimeter and the samples is a more invasive procedure than using the smartphone method.

In terms of smartphone advantages, the proposed setup is less time consuming, since only a photograph can contain the information about a big area of the sample, while the sampling process with the reference device needs to be done one spot at a time. Finally, the proposed smartphone setup is economically more sustainable than the spectrocolorimeter, especially if employed as a first screening approach before running more expensive, invasive and time-consuming techniques.

Smartphone application in roman fresco wall painting

The proposed setup, schematically represented in Fig. 5, has shown to work efficiently in classifying three different pigments (and their mixtures) based on CIE L*a*b* colour parameters. The feasibility of the method requires a constant distance from the camera sensor to the wall, as well as a parallel position of the smartphone to the surface in order to properly record colour. Additionally, since the colour measurement can be altered by the position in the photograph, the reference colour sheet must be close to the coloured spot under investigation, avoiding to distort the colour measurement. Once captured, a simple image analysis step is required, including the data processing in the SVC model in order to identify the pigment. To obtain reliable results, lighting conditions should be controlled providing homogeneous illumina-

Table 5
Confusion matrix for the SVC ($k = 1$, $C = 15$) model created with pure pigments as calibration and mixtures as test samples. Colorimetric data of CIE L*a*b*.

Real	Predicted *0.2Fe_0.6Hg*	*0.2Fe_0.6Pb*	*0.2Hg_0.6Pb*	*0.6Fe_0.2Hg*	*0.6Fe_0.2Pb*	*0.6Hg_0.2Pb*	cinnabar	haematite	minium
0.2Fe_0.6Hg	5	0	0	0	0	0	0	0	0
0.2Fe_0.6Pb	0	5	0	0	0	0	0	0	0
0.2Hg_0.6Pb	0	0	5	0	0	0	0	0	0
0.6Fe_0.2Hg	0	0	0	4	1	0	0	0	0
0.6Fe_0.2Pb	0	0	0	0	5	0	0	0	0
0.6Hg_0.2Pb	0	0	0	0	0	5	0	0	0
cinnabar	0	0	0	0	0	0	23	0	0
haematite	0	0	0	0	0	0	1	23	2
minium	0	0	0	0	0	0	0	3	21

tion in both the painting surface and to the reference sheet. The sampling strategy should be developed considering the conservation state and the colour intensity of the samples. Also, archaeological information about the context is required to ensure that the pigments under investigation are likely to be either haematite, minium or cinnabar (or a mixture of those). Otherwise, the classification method would classify the sample as the pigment which is the most similar amongst the ones included in the calibration step.

Overall, the proposed smartphone application was especially designed to identify red colour in *frescoes* and could be easily employed as a screening method by non-specialists. Furthermore the method could be implemented and be tested in other range of colours employed in ancient artwork.

Conclusions

In this work, a new analytical approach using smartphone to classify different compounds used as red pigments in *frescoes* has been successfully developed. Portable X-ray fluorescence, Fourier Transform Infrared spectroscopy, Raman spectroscopy and visible reflectance spectroscopy were used as reference methods, and the obtained results were cross-referenced with the smartphone ones, showing the reliability of the proposed methodology. Smartphone colorimetry and image data processing were used to obtain an easy and fast analytical tool applied to the Cultural Heritage field. To ensure the in-field applicability of the methodology, the colorimetric data obtained with a smartphone device (in the CIE L*a*b* colour space) was calibrated using a reference colour sheet to compensate for the lighting conditions variability. Using the colorimetric dataset parameters, three different classificatory models were created: kNN, LDA and SVC. LDA and SVC proved to work more efficiently than kNN, returning lower classification errors. Comparing LDA and SVC, both worked pretty similarly in terms of classification, with 7.70% and 6.80% errors respectively. Furthermore, mixtures of different red pigment samples were successfully classified as the respective combination of colours.

Thus, the application of SVC is recommended, given that its computational cost is very small, and that it has proven to yield the lowest errors of prediction under these conditions. Additionally, this algorithm can be easily applied in free access software like R.

Since this procedure uses corrected data rather than raw RGB parameters directly extracted from the smartphone, the representation of colour is not affected by lighting conditions, one of the main drawbacks of using smartphone colorimetry rather than a reference device. Also, from the point of view of time, the proposed setup in is less time consuming, since a single photograph contains colour information for many different spots, while for colorimeter every spot of interest needs to be measured. Furthermore, a big advantage of the proposed approach lays on the fact that colorimeters usually have a reduced radius of measurement, which depends on the device, (usually 1–2 cm in diameter) and usually a direct contact with the sample is needed. Also, in some cases where colour is depicted in very narrow lines, or small spots, the smartphone approach allows to select information of only a few pixels, being able to go further in a detailed analysis.

This work demonstrates the applicability of the digital image colorimetry using smartphones, coupled with chemometric tools, in the field of Cultural Heritage analysis. For the first time, an analytical approach for the qualitative identification of red pigments in frescoes has been developed using digital smartphone colorimetry. To it, a dataset must be created in order to generate the predictive models, and then new samples be predicted. In this sense, the dataset created in this work is available upon request to the authors, although, creating a dataset and capturing colour parameters of the samples with the same device that will be used in the field, is suggested.

With it, a previous scan of the wall paintings can be carried out and quickly assessed employing the easy and low-cost materials that are described in this study. However, as this procedure relays on the reflected colour of the surface, it must be considered that potential errors might arise from shining (due to some protective covering of the fresco) and/or from polluting agents deposited on the wall, like could be the case of carbon or dirt incrustations. In such cases, colour should be recorded after the artwork restoration.

Finally, this paper has demonstrated that historical red pigments used in *frescoes* can be identified by smartphone digital image colorimetry, and hence constitutes the foundations to develop a future application which allows to assign a specific colour with the corresponding historical pigment used. To it, further investigations will be needed so as to study other common colours and hues.

Acknowledgements

This project has been funded by the Conselleria d'Innovació, Universitats, Ciència i Societat Digital, Generalitat Valenciana (PROMETEO-2019–056). Roberto Sáez-Hernández thanks the Ministry of Universities of Spain for a predoctoral FPU/19/02304 position, and Mirco Ramacciotti for his advice during the work. Gianni Gallello acknowledges the financial support of the Beatriz Galindo Fellowship (2018) funded by the Spanish Ministry of Universities (Project BEAGAL18/00110 "Development of analytical methods applied to archaeology").

Supplementary materials

Supplementary material associated with this article can be found, in the online version, at doi:10.1016/j.culher.2022.10.003.

References

[1] A. Adriaens, Non-destructive analysis and testing of museum objects: an overview of 5 years of research, Spectrochim. Acta Part B At. Spectrosc. 60 (2005) 1503–1516, doi:10.1016/J.SAB.2005.10.006.
[2] J. Tuñón, A. Sánchez, D.J. Parras, P. Amate, M. Montejo, B. Ceprián, The colours of Rome in the walls of Cástulo (Linares, Spain), Sci. Reports 10 (2020) 1–15 2020 101, doi:10.1038/s41598-020-69334-y.
[3] C. Boschetti, A. Corradi, P. Baraldi, Raman characterization of painted mortar in Republican Roman mosaics, J. Raman Spectrosc. 39 (2008) 1085–1090, doi:10.1002/JRS.1970.
[4] M. Romani, G. Capobianco, L. Pronti, F. Colao, C. Seccaroni, A. Puiu, A.C. Felici, G. Verona-Rinati, M. Cestelli-Guidi, A. Tognacci, M. Vendittelli, M. Mangano, A. Acconci, G. Bonifazi, S. Serranti, M. Marinelli, R. Fantoni, Analytical chemistry approach in cultural heritage: the case of Vincenzo Pasqualoni's wall paintings in S. Nicola in Carcere (Rome), Microchem. J. 156 (2020) 104920, doi:10.1016/J.MICROC.2020.104920.
[5] I. Aliatis, D. Bersani, E. Campani, A. Casoli, P.P. Lottici, S. Mantovan, I.-.G. Marino, Pigments used in Roman wall paintings in the Vesuvian area, J. Raman Spectrosc. 41 (2011) 1537–1542, doi:10.1002/JRS.2701.
[6] N. Prieto-Taboada, S.F.-O. de Vallejuelo, A. Santos, M. Veneranda, K. Castro, M. Maguregui, H. Morillas, G. Arana, A. Martellone, B. de Nigris, M. Osanna, J.M. Madariaga, Understanding the degradation of the blue colour in the wall paintings of Ariadne's house (Pompeii, Italy) by non-destructive techniques, J. Raman Spectrosc. 52 (2021) 85–94, doi:10.1002/JRS.5941.
[7] C.J. Lin, Y.T. Prasetyo, N.D. Siswanto, B.C. Jiang, Optimization of color design for military camouflage in CIELAB color space, Color Res. Appl. 44 (2019) 367–380, doi:10.1002/COL.22352.
[8] P.B. Pathare, U.L. Opara, F.A.J. Al-Said, Colour measurement and analysis in fresh and processed foods: a review, Food Bioprocess Technol 6 (2013) 36–60, doi:10.1007/s11947-012-0867-9.
[9] A. Paradisi, A. Sodo, D. Artioli, A. Botti, D. Cavezzali, A. Giovagnoli, C. Polidoro, M.A. Ricci, Domus aurea, the "sala delle maschere": chemical and spectroscopic investigations on the fresco paintings, Archaeometry 54 (2012) 1060–1075, doi:10.1111/j.1475-4754.2012.00678.x.
[10] S. Pagès-Camagna, S. Colinart, The Egyptian green pigment: its manufactering process and links to Egyptian blue, Archaeometry 45 (2003) 637–658, doi:10.1046/J.1475-4754.2003.00134.X.

[11] O. Hahn, D. Oltrogge, H. Bevers, Coloured prints of the 16th century: non-destructive analyses on coloured engravings from albrecht dürer and contemporary artists, Archaeometry 46 (2004) 273–282, doi:10.1111/J.1475-4754.2004.00157.X.
[12] G. Capobianco, G. Agresti, G. Bonifazi, S. Serranti, C. Pelosi, Yellow pigment powders based on lead and antimony: particle size and colour hue, J. Imaging. 7 (2021) 127, doi:10.3390/JIMAGING7080127.
[13] P. Modarresi, R. Jafari, S. Noghani, Recognition of vermilion preparation methods in Safavid illustrated manuscripts through colorimetric analysis, Archaeometry. (2021). https://doi.org/10.1111/ARCM.12677.
[14] Y. Fan, J. Li, Y. Guo, L. Xie, G. Zhang, Digital image colorimetry on smartphone for chemical analysis: a review, Measurement 171 (2021) 108829, doi:10.1016/J.MEASUREMENT.2020.108829.
[15] L.F. Capitán-Vallvey, N. López-Ruiz, A. Martínez-Olmos, M.M. Erenas, A.J. Palma, Recent developments in computer vision-based analytical chemistry: a tutorial review, Anal. Chim. Acta. 899 (2015) 23–56, doi:10.1016/j.aca.2015.10.009.
[16] L.J. Loh, G.C. Bandara, G.L. Weber, V.T. Remcho, Detection of water contamination from hydraulic fracturing wastewater: a μpAD for bromide analysis in natural waters, Analyst 140 (2015) 5501–5507, doi:10.1039/c5an00807g.
[17] J. Dou, J. Shang, Q. Kang, D. Shen, Field analysis free chlorine in water samples by a smartphone-based colorimetric device with improved sensitivity and accuracy, Microchem. J. 150 (2019) 104200, doi:10.1016/j.microc.2019.104200.
[18] R. Sáez-Hernández, A.R. Mauri-Aucejo, A. Morales-Rubio, A. Pastor, M.L. Cervera, Phosphate determination in environmental, biological and industrial samples using a smartphone as a capture device, New J. Chem. 46 (2022) 1286–1294, doi:10.1039/D1NJ05425B.
[19] R. Sáez-Hernández, K.U. Antela, A.R. Mauri-Aucejo, A. Morales-Rubio, M.L. Cervera, Smartphone-based colorimetric study of adulterated tuna samples, Food Chem 389 (2022) 133063, doi:10.1016/J.FOODCHEM.2022.133063.
[20] M. de O.K. Franco, W.T. Suarez, V.B. dos Santos, I.S. Resque, A novel digital image method for determination of reducing sugars in aged and non-aged cachaças employing a smartphone, Food Chem 338 (2021) 127800, doi:10.1016/j.foodchem.2020.127800.
[21] Y. Cui, T. Chen, B. Li, X. Liu, J. Xia, J. Han, Y. Wu, M. Yang, Colorimetric sensor array–smartphone–remote server coupling system for rapid detection of saccharides in beverages, J. Iran. Chem. Soc. 15 (2018) 1085–1095, doi:10.1007/s13738-018-1306-2.
[22] M. Ramacciotti, G. Gallello, M. Lezzerini, S. Pagnotta, A. Aquino, L. Alapont, J.A. Martín Ruiz, A. Pérez-Malumbres Landa, R. Hiraldo Aguilera, D. Godoy Ruiz, A. Morales-Rubio, M.L. Cervera, A. Pastor, Smartphone application for ancient mortars identification developed by a multi-analytical approach, J. Archaeol. Sci. Reports. 43 (2022) 103433, doi:10.1016/J.JASREP.2022.103433.
[23] R. Piovesan, C. Mazzoli, L. Maritan, P. Cornale, Fresco and lime-paint: an experimental study and objective criteria for distinguishing between these painting techniques, Archaeometry 54 (2012) 723–736, doi:10.1111/J.1475-4754.2011.00647.X.
[24] M.K. Neiman, M. Balonis, I. Kakoulli, Cinnabar alteration in archaeological wall paintings: an experimental and theoretical approach, Appl. Phys. A. 121 (2015) 915–938, doi:10.1007/S00339-015-9456-X.
[25] L. Regazzoni, G. Cavallo, D. Biondelli, J. Gilardi, Microscopic analysis of wall painting techniques: laboratory replicas and romanesque case studies in southern Switzerland, Stud. Conserv. 63 (2018) 326–341, doi:10.1080/00393630.2017.1422891.
[26] T. Hastie, R. Tibshirani, G. James, D. Witten, An Introduction to Statistical Learning, 2nd Ed., Springer, 2021 https://www.statlearning.com/.
[27] F. Marini, Classification methods in chemometrics, Curr. Anal. Chem. 6 (2010) 72–79, doi:10.2174/157341110790069592.
[28] J. Luts, F. Ojeda, R. Van de Plas Raf, B. De Moor, S. Van Huffel, J.A.K. Suykens, A tutorial on support vector machine-based methods for classification problems in chemometrics, Anal. Chim. Acta. 665 (2010) 129–145, doi:10.1016/J.ACA.2010.03.030.
[29] Y. Xu, S. Zomer, R.G. Brereton, Support vector machines: a recent method for classification in chemometrics, Crit. Rev. Anal. Chem. 36 (2006) 177–188, doi:10.1080/10408340600969486.
[30] L. Abad-Casal, Pintura Romana En España - I, Universidad de Alicante & Universidad de Sevilla, Cádiz, 1982 http://rua.ua.es/dspace/handle/10045/21902#vpreview.
[31] P. Olmos-Benlloch, La preparación de la pintura mural en el mundo romano, Ex Novo Rev. d'història i Humanit. 3 (2006) 23–40 https://raco.cat/index.php/ExNovo/article/view/144713.
[32] C. Guiral-Pelegrín, Pinturas murales romanas procedentes del Grau Vell (Sagunto, Valencia), Sagvntum. 25 (1992) 139–178, doi:10.7203/SAGVNTVM..3643.
[33] J. Cuní, What do we know of Roman wall painting technique? Potential confounding factors in ancient paint media analysis, Herit. Sci. 4 (2016) 1–13, doi:10.1186/S40494-016-0111-4.
[34] J. Tuñón, A. Sánchez, D.J. Parras, P. Amate, M. Montejo, B. Ceprián, The colours of Rome in the walls of Cástulo (Linares, Spain), Sci. Rep. 10 (2020) 1–15, doi:10.1038/s41598-020-69334-y.
[35] M.L. Vitruvio Polion, Los Diez Libros de arquitectura, Alianza Forma 400 (1997) https://www.u-cursos.cl/fau/2015/0/AO104/1/foro/r/1_Vitrubio_Los_diez_Libros_de_Architectura.pdf.
[36] P. Westlake, P. Siozos, A. Philippidis, C. Apostolaki, B. Derham, A. Terlixi, V. Perdikatsis, R. Jones, D. Anglos, Studying pigments on painted plaster in Minoan, Roman and Early Byzantine Crete. A multi-analytical technique approach, Anal. Bioanal. Chem. 402 (2012) 1413–1432, doi:10.1007/S00216-011-5281-Z.
[37] E.J. Cerrato, D. Cosano, D. Esquivel, C. Jiménez-Sanchidrián, J.R. Ruiz, Spectroscopic analysis of pigments in a wall painting from a high Roman Empire building in Córdoba (Spain) and identification of the application technique, Microchem. J. 168 (2021) 106444, doi:10.1016/J.MICROC.2021.106444.
[38] J. Malo, M.J. Luque, COLORLAB: color science in matlab, (2002). http://www.uv.es/vista/vistavalencia/software.html (accessed May 25, 2021).
[39] R. Core-Team, R: a language and environment for statistical computing, (2021). https://www.r-project.org/.
[40] A. Kassambara, F. Mundt, factoextra: extract and Visualize the Results of Multivariate Data Analyses, (2020). https://cran.r-project.org/package=factoextra (accessed October 13, 2021).
[41] W.N. Venables, B.D. Ripley, Modern Applied Statistics With S, 4th Ed., Springer, New York, 2002.
[42] D. Meyer, E. Dimitriadou, K. Hornik, A. Weingessel, F. Leisch, e1071: misc functions of the department of statistics, probability theory group (Formerly: E1071), (2021). https://cran.r-project.org/package=e1071.
[43] J.J. Sebastien Le, F. Husson, FactoMineR: an R Package for Multivariate Analysis, J. Stat. Softw. 25 (2008) 1–18 https://www.jstatsoft.org/article/view/v025i01.
[44] H. Wickham, ggplot2: elegant Graphics for Data Analysis, (2016).
[45] signal: Signal processing, (2013). http://r-forge.r-project.org/projects/signal/.
[46] N. Kumar, A. Bansal, G.S. Sarma, R.K. Rawal, Chemometrics tools used in analytical chemistry: an overview, Talanta 123 (2014) 186–199, doi:10.1016/J.TALANTA.2014.02.003.
[47] M. Pohar, M. Blas, S. Turk, Comparison of logistic regression and linear discriminant analysis, Metod. Zv. 1 (2004) 143–161, doi:10.51936/ayrt6204.
[48] Å. Rinnan, F. van den Berg, S.B. Engelsen, Review of the most common preprocessing techniques for near-infrared spectra, TrAC - Trends Anal. Chem. 28 (2009) 1201–1222, doi:10.1016/j.trac.2009.07.007.
[49] Calcium carbonate (precipitated), (n.d.). https://webbook.nist.gov/cgi/cbook.cgi?ID=C471341&Mask=80 (accessed January 28, 2022).
[50] V.H.J.M. dos Santos, D. Pontin, G.G.D. Ponzi, A.S. de G. e. Stepanha, R.B. Martel, M.K. Schütz, S.M.O. Einloft, F. Dalla Vecchia, Application of Fourier Transform infrared spectroscopy (FTIR) coupled with multivariate regression for calcium carbonate (CaCO3) quantification in cement, Constr. Build. Mater. 313 (2021) 125413, doi:10.1016/J.CONBUILDMAT.2021.125413.
[51] H. Böke, S. Akkurt, S. Özdemir, E.H. Göktürk, E.N. Caner Saltik, Quantification of CaCO3–CaSO3·0·5H2O–CaSO4·2H2O mixtures by FTIR analysis and its ANN model, Mater. Lett. 58 (2004) 723–726, doi:10.1016/J.MATLET.2003.07.008.
[52] S. Kraft, E. Knittle, Q. Williams, Carbonate stability in the Earth's mantle: a vibrational spectroscopic study of aragonite and dolomite at high pressures and temperatures, J. Geophys. Res. Solid Earth. 96 (1991) 17997–18009, doi:10.1029/91JB01749.
[53] R. Ylmén, U. Jäglid, Carbonation of portland cement studied by diffuse reflection fourier transform infrared spectroscopy, Int. J. Concr. Struct. Mater. 7 (2013) 119–125, doi:10.1007/s40069-013-0039-y.
[54] E. Catelli, G. Sciutto, S. Prati, R. Mazzeo, MID-FTIR macro mapping and clustering-based automatic brushing: an advanced diagnostic tool for in situ investigations of artworks, Proceeding SPIE 26 (2019), doi:10.1117/12.2526117.
[55] G. Ramis Ramos, M.C. García Álvarez-Coque, Quimiometría, Síntesis, Madrid, 2001.
[56] T. Hastie, R. Tibshirani, G. James, D. Witten, An Introduction to Statistical Learning, G. Casella, Springer, 2006.